JAST, Vol. 2, No. 3, pp 9–18

JAST
Journal of Aerospace Science and Technology

Trajectory Optimization of a Multi Stage Launch Vehicle Using Nonlinear Programming

S. Serpooshan[1], A. Naghash[2]

This work is an example for application of nonlinear programming for the problem of three- dimensional trajectory optimization of multi-stage launch vehicles for geostationary orbit missions. The main objective is to minimize fuel consumption or equivalently to maximize the payload. The launch vehicle studied here, Europa- II, consists of 5 thrust phases and 2 coast phases. The major parameters of the coast arcs such as inclination, eccentricity and true anomaly of attachment points are not prespecified and should be found in the optimization problem. The fairing should be jettisoned whenever aerothermal flux falls below a certain value. A maximum aerodynamic heating constraint for the atmospheric part of the flight is also considered. The problem is solved with the direct collocation method and results are compared with those in Ref. 1 (W.Duffek, G.C.Shau), where an indirect multiple shooting method with an inner loop for parameter optimization is used. Advantages of present work with respect to methods used in specified references are then discussed.

NOMENCLATURE

A	aerodynamic force
a	major semi-axis of an orbit
a_T	major semi-axis of transfer orbit
C	defect constraints
C_D	drag coefficient
C_1	aerodynamic heating index
C_2	maximum permissible value for heat rate
e	eccentricity
f	state equation
g	Earth's gravitational acceleration
h	height (geocentric altitude), r-R_E
h_{AT}	apogee height of transfer orbit
h_{PT}	perigee height of transfer orbit
h_t	time step size for discretization
i	inclination
i_C	inclination of coast orbit (C.O.)
i_T	inclination of transfer orbit (T.O.)
I_{sp}	specific impulse
J	performance index
J_2	flattening coefficient of the Earth potential
m	mass
m_P	vehicle mass in primary orbit
m_T	vehicle mass in transfer orbit
q	dynamic pressure
Q	kinetic energy of the inflow per unit area
r	distance from the Earth center
R_α^x	rotation matrix (rotation α about x axis)
R_E	equatorial radius of the Earth
t	time or beginning time
$t_{2,3,4}$	beginning time of stages 2, 3 or 4
t_C	beginning time of coast phase
t_f	final time or time of burnout
t_{f4}	burnout of stage 4
t_s	separation time of fairing
T_C	temperature rise of critical points of the vehicle
T	thrust

1. *Graduate Student, Department of Aerospace Engineering, 19536-45763, Amirkabir University of Technology, Tehran.*
2. *Assistant Professor, Department of Aerospace Engineering, 15875-4413, Amirkabir University of Technology, Tehran*

V	velocity
V_{AT}	vehicle velocity at apogee of transfer orbit
V_{AP}	velocity required at apogee of primary orbit
α	angle of attack
β	side slip angle
γ	flight path angle
δ	geocentric latitude angle
δ_L	launching point latitude
Δa	perturbation in major semi-axis
Δe	perturbation in eccentricity
Δt	phase duration
ΔV	velocity increment
ϵ	thrust direction angle, horizontal (Figure 2)
ν	true anomaly
θ	longitude angle with respect to the launching meridian
θ_4	θ at the beginning of the 4^{th} stage
θ_g	geographical longitude
μ_E	the gravitation number of the Earth
σ	thrust direction angle, vertical (Figure 2)
χ	azimuth angle (clockwise from the North)
χ_0	launching azimuth angle
χ_0^*	optimal value for launching azimuth
ω_E	angular velocity of the Earth

Subscripts

C	coast phase orbit (first coast arc)
b	body coordinate system (vehicle-fixed)
f	due to final time
G	geostationary orbit
h	local horizontal coordinate system
i	inertial coordinate system
$i.j$	index of state equations
P	primary orbit
T	transfer orbit
w	velocity (wind) coordinate system

Superscripts

k	time index
x, y, z	force components in x, y or z direction

INTRODUCTION

The present work is an investigation on the problem of optimizing the ascent trajectory of a 4-stage launch vehicle including operational constraints. The launch vehicle under consideration, Europa-II, was developed and constructed by European Launcher Development Organization (ELDO) for the purpose of bringing communication satellites into the Geostationary Earth Orbit (GEO).

The launch vehicle performance, which is usually the percentage of the total mass that can be used as payload, depends first on staging mass ratios and then on how to guide the vehicle to minimize fuel consumption or, equivalently, to attain maximum payload in the desired orbit. Here, the performance index is defined as delivered mass into a target orbit. This mass is made up of a satellite and a residual quantity of fuel that can be used to maintain the satellite in that orbit (about 4 kg/year). The target orbit can be chosen as a primary orbit that is attached to the geostationary one. So, the main objective of this work is to maximize the final mass in the primary orbit (P.O.) without any technical change of the vehicle and with all given constraints.

The ascent trajectory consists of 5 thrust phases and 2 coast phases. The first coast phase is next to the third stage, and the other, called transfer orbit, is followed by the fourth stage. Figure 1 shows the plan of the trajectory. The thrust propelled phases are shown by numbers 1 to 5, and the trajectory path is shown in dark. As it is shown, attachment point to the transfer orbit (i.e. burnout of stage 4) is not necessarily at perigee point.

The vehicle is launched from Kourou in French Guiana space center. This site offers an equatorial latitude (Table 3) to maximize launch velocities and a wide azimuth of over ocean launch trajectories preventing overfly of population centers. The first three stages lead the vehicle into the first coast phase orbit (C.O.) where it follows a free flight as far as the equator. The

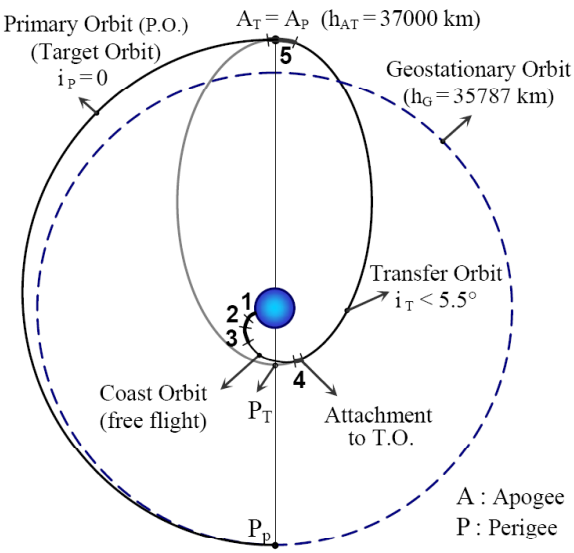

Figure 1. The Schematic Plan of Trajectory

Table 1. Nominal mass-time balance of the vehicle

Phase	t(s)	Δt(s)	m_{0total} (kg)	$m_{structure}^{jettisoned}$ (kg)	m_{Fuel}(kg)	$\dot{m}_{Fuel}$(kg/s)	I_{SP}(s)	Thrust(kN)
0	0	10	112099.0	-	8402.9	549.1641	247.779	1334.315
1	10	150.9772	106607.36	6175.3	82911.3		I_{SP} = f(h)	T = f(h)
2a	160.9772 + 2.9745	102.8490	17520.8	330 (fairing)	9853.6	95.8065	280.889	263.889
2b	t_s=Optimal		f(t_s)	2409.1				
3	266.8007 + 2.6014	354.8456	4928.1	0	2773.1 + 43.7	7.9381	300.230	23.370
C.O.	624.2477	Δt_C=Free	2111.3	937	-	-	-	0
4	t_4=t_3+Δt_C	45	1174.3	101.9	685.4	15.2311	275.498	41.147
T.O.	t_4 + 45	Free	387.0	-	-	-	-	0
5		Impulse-Like	387.0		f(ΔV_5) = Min.		302.121	

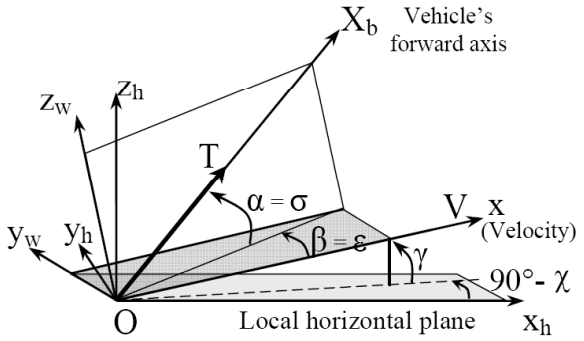

Figure 2. Main Coordinate Systems and Angles

4^{th} stage then shoots it into the transfer orbit (T.O.) which is the second free flight phase, transfering the vehicle from its low altitudes (usually below 500 km) to the apogee height of primary orbit (37000 km). At the end of this phase, i.e. in the apogee area of the transfer orbit, the apogee engine shoots the vehicle into the primary orbit. This is called the fifth thrust phase. The apogee system eliminates the inclination and eccentricity of the transfer orbit, and corrects the satellite positions above the equator. As is shown in Figure 1, the primary orbit is attached to the transfer orbit at its apogee, and attains the GEO height at its perigee with zero inclination.

THE LAUNCH VEHICLE SPECIFICATIONS

EUROPA-II space vehicle specifications are described here. This vehicle is regarded as a point-mass. The control parameters to be found as optimal are thrust direction angles σ, ϵ defined in the velocity axis system. As shown in Figure 2, the thrust vector lies along the longitudinal axis of the vehicle. Therefore, control angles are the same as the angle of attack and side-slip (wind effects are not taken into consideration). The main events and nominal properties of the stages are listed in Table 1. There are small delay times between the burnout of each stage and the ignition of the next stage (2.9745 sec. after stage 1 and 2.6014 sec. after stage 3), which should be taken into consideration.

During the first stage, the specific impulse of engines depends on the flight height due to variation of the back pressure at different altitudes. The flight of the first stage proceeds along an Earth-fixed great plane, which passes through the launching point. The reserve propellant of third stage (43.7 kg), which serves to correct the expected dispersions of the trajectory and permit a tolerance in the payload is assumed to be consumed.

Control and guidance of the vehicle is applied through an internal guidance system, which consists of an inertial platform, a guidance and control computer, and a thrust direction setting and adjusting system. The guidance computer uses the prespecified guidance law and measured values of the inertial platform to produce a closed-loop control system that makes it possible to implement arbitrary attitude angle programs. In the first stage, the vehicle uses gravity turn guidance pitch program to minimize aerodynamic heat loads (as it causes a zero angle of attack trajectory). All engines have a constant fuel mass flow rate, and can be ignited only once. For the purpose of calculating the specified performance index, it can be assumed that the apogee engine which is infact the fifth stage, provides an impulse-like thrust at the apogee point of the transfer orbit.

The payload is protected from high temperatures by the sheathing located in the head of the vehicle called payload fairing. This fairing is jettisoned at an optimal time during the 2^{nd} stage.

CONSTRAINTS

Aerodynamic Heating

The stagnation point heat rate is a measure for the amount of energy that the ambient medium will dissipate to the vehicle at any unit of time. From Ref. (7), it is given by:

$$\dot{Q} = C\rho^n V^m = \frac{1}{2}\rho V^3 \qquad (1)$$

where the substituted values for parameters (C=1/2, n=1, and m=3) are for free stream enthalpy assumptions. The large amount of aerodynamic heating produced in the atmospheric part of the ascent flight, causes a high temperature rise in the outer surfaces and critical points of the vehicle. It is too difficult to predict the generated temperature distribution and variable temperature stresses in the structure of the vehicle. So, aerodynamic heating is usually taken into account by the help of other parameters, e.g. dynamic pressure, (see [3]), and are easy to calculate. In the present work, the constraint due to aerodynamic heating is defined as below:

$$Q(t) = \int_0^t \dot{Q} dt \leq Q_{max} \tag{2a}$$

$$\int_0^t \frac{1}{2}\rho V^3 dt \leq C_1 \tag{2b}$$

For the current vehicle, the maximum permissible value of the constant C_1 (for trajectories with a zero angle of attack) is given as 140 kJ/cm^2 [1]. This constant is referred to as the heating index. Most of this energy will be radiated into the ambient, only a small fraction is actually conducted through the insulation. To each value of the heating index C_1, there correspond particular temperature rises at critical points of the vehicle structure, which must not exceed certain limits. According to the calculations made by ELDO [1], the following correlation exists between the heating index and the temperature rise of the critical points: Another constraint due to the aerodynamic heating is the maximum heat rate. The fairing should be jettisoned during the 2^{nd} stage whenever the aerothermal flux (heat rate) falls below a certain value (C_2), and the heat rate should not exceed this value afterwards:

$$\frac{1}{2}\rho V^3 = C_2, \quad t = t_s \tag{3a}$$

$$\frac{1}{2}\rho V^3 \leq C_2, \quad t \geq t_s \tag{3b}$$

Here, the permissible value of C_2 is 0.1 W/cm^2 [1]. If the fairing separates soon, the remaining portion of the trajectory should be such that the heat rate is kept below a specific value, which acts as a new limitation that decreases the performance. On the other hand, if this separation occurs too late, the vehicle should carry the weight of sheathing for a long time, which again decreases the performance. Thus, there is an optimal separation time (t_s) that should be found. Because the air density is too low at altitudes higher than 150 km, Eq. (3b) may be stated in other words: The vehicle must not dip below the specified height when the fairing has been jettisoned. This latter condition is called "minimum dip-in height" and is used in [1]. However, because this condition is not always true and depends on the velocity, Eq. (3b) is preferred and used here.

Table 2. Effect of Heating Index on Temperature

C_1 (kJ/cm^2)	130	140	160	180
Temperature rise (°C)	213	232	269	305

Table 3. Geographical Locations

	δ, deg	θ_g, deg	h, m
Launch site (Kourou)	+5.2366 (N)	-52.7753 (W)	0.0
Brazzaville station	-4.191 (S)	+15.250 (E)	+40.0

Launching Azimuth Limitation

Due to safety considerations, the trajectory of the launch vehicle in the first stage should occurr within a great plane that passes from the launching point and forms an angle of 91.6° with the local North there (C.W. direction) i.e.

$$\chi_{(t)} = \chi_0 = 91.6°, \quad t \in [0, t_{f1}] \tag{4}$$

EQUATIONS OF MOTION

The launch vehicle is modeled as a 3DOF point-mass model. From [4], the state equations of motion in the

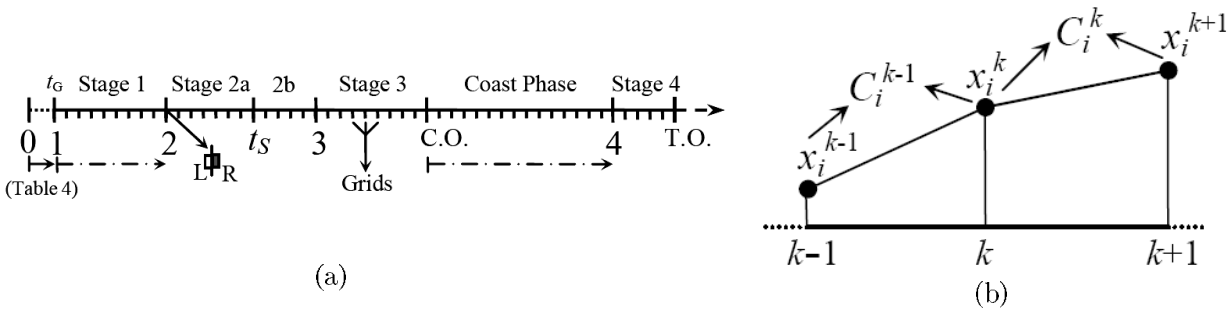

Figure 3. (a)Discretization, (b)Defects

velocity coordinate system are:

$$\dot{\theta} = V_r \sin\chi / \cos\delta \tag{5a}$$

$$\dot{\delta} = V_r \cos\chi \tag{5b}$$

$$\dot{r} = V \sin\gamma \tag{5c}$$

$$\dot{V} = u_E w_E(\cos\delta\sin\gamma - \sin\delta\cos\gamma\cos\chi) - g\sin\gamma + (T/m)\cos\sigma\cos\varepsilon + A_w^x/m \tag{5d}$$

$$\dot{\chi} = V_r \sin\chi\tan\delta + 2\omega_E(\sin\delta - \cos\chi\cos\delta\tan\gamma) + [u_E\sin\chi\sin\delta - (T/m)\cos\sigma\sin\varepsilon - A_w^y/m]/(V\cos\gamma) \tag{5e}$$

$$\dot{\gamma} = V_r + 2\omega_E\sin\chi\cos\delta + (u_E w_E/V)(\cos\delta\cos\gamma + \sin\delta\sin\gamma\cos\chi) - [g\cos\gamma + (T/m)\sin\sigma + A_w^z/m]/V \tag{5f}$$

where A_w terms are components of aerodynamic forces (described in the next section) in the velocity axis system and V_r and u_E are defined as:

$$V_r \equiv (V/r).cos\gamma \tag{6}$$

$$u_E \equiv r\omega_E\cos\delta. \tag{7}$$

The thrust is given by:

$$T = g.I_{SP}.\dot{m}_{Fuel}. \tag{8}$$

All fuel mass flow rates and specific impulses (except for the first stage) are constant values as given in Table 1. The height dependency of the specific impulse in the first stage is given by:

$$I_{SP(1)} = k_1 - k_2.\exp(-k_3.h). \tag{9}$$

As the trajectories under consideration lie in the vicinity of the equator plane ($|\delta| < 5.5°$), for geometrical purposes such as geometric height and geographic latitude, the Earth is regarded as a sphere. However, the polar flattening of the Earth is taken into account for gravity:

$$g(r) = (\mu_E/r^2)[1 + (3/2)J_2(R_E/r)^2]. \tag{10}$$

AERODYNAMIC AND ATMOSPHERIC DATA

The aerodynamic forces exist only in the atmospheric part of the ascent i.e. at the first stage. The roll angle always remains zero during the flight in the Earth-fixed great plane of the first stage. These forces depend on the Mach number, angle of attack and the side-slip angle. The aerodynamic coefficients are given in the tabular form in [1]. Although, approximations in the form of exponential and polynomial functions are given in [1], the cubic-spline method is used here.

The atmospheric data such as air density and

Table 4. Coefficients of Eq.(9)

k_1(s)	k_2(s)	k_3(s)
284.359	36.58	1.44E-4

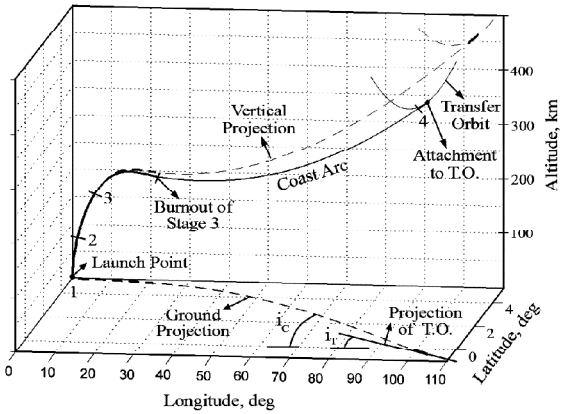

Figure 4. Ascent to transfer orbit (Free Attachment, B)

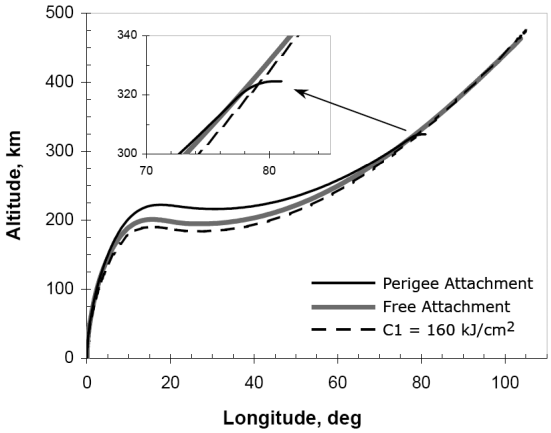

Figure 5. Time histories of altitudes

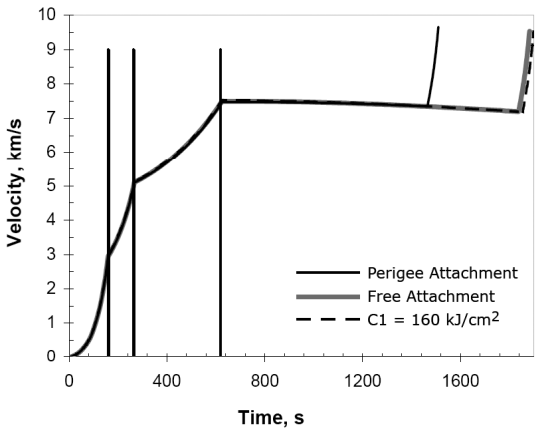

Figure 6. Time histories of velocities

sound speed are approximated by appropriate analytical functions of the U.S. standard atmosphere [5]. Wind effects are not considered in the mathematical model.

PROBLEM STATEMENT

This section formulates the problem. State and control vectors are defined as:

$$\vec{X} = [\theta, \delta, r, V, \chi, \gamma, Q, m]^T \tag{11}$$

$$\vec{U} = [\sigma, \epsilon]^T. \tag{12}$$

Differential equations of states are given by Eqs. (5a) to (5f), (1) and (13):

$$\dot{m} = -\dot{m}_{Fuel}. \tag{13}$$

The mass has jumps at the stages separation and also at the jettisoning of the fairing.

The right hand boundary of the optimization problem is at the burnout of the 4^{th} stage i.e. when the vehicle enters the transfer orbit. To specify the necessary conditions for T.O. entrance, it is necessary to find the inertial values of V, χ and γ from the states in the velocity coordinate system which are relative to the Earth. The inertial parameters are given by:

$$V_i^2 = V^2 + u_E^2 + 2u_E V_\chi \tag{14a}$$

$$\sin\chi_i = (V_\chi + u_E)/(V^2\cos^2\gamma + u_E^2 + 2u_E V_\chi)^{1/2} \tag{14b}$$

$$\sin\gamma_i = V\sin\gamma/V_i \tag{14c}$$

where u_E is defined by Eq. (7) and V_χ is defined as:

$$V_\chi \equiv V\cos\gamma\sin\chi. \tag{15}$$

Performance Index

As already stated, it is interesting to maximize the vehicle mass in the primary orbit. Transferring this into a minimization problem yields the cost function as:

$$J = -m_P/m_{ref}, \tag{16}$$

Here, m_{ref} is a constant to scale the J. Since the 5^{th} thrust phase in the apogee area of T.O. is assumed to be impulse-like, we can write:

$$m_P = m_T.\exp(-\Delta V_5/(g.I_{SP5})). \tag{17}$$

where ΔV_5 is the velocity increment required for entry into the primary orbit and is found from:

$$\Delta V_5 = |\vec{V}_{AP} - \vec{V}_{AT}| = \sqrt{V_{AT}^2 + V_{AP}^2 - 2V_{AT}V_{AP}\cos(i_T)} \tag{18}$$

During the flight in transfer orbit, the potential by non-spherical Earth i.e. effect of J_2 term in Earth gravity disturbs the keplerian elements of the orbit. The parameters a, e of T.O. (and therefore of P.O.) are corrected at the apogee point by simplified equations of gravitational perturbations given by Kozai [6]. For the flight from the perigee to the apogee we can write [1]:

$$\overset{0\to\pi}{\Delta a} = J_2(R_E^2/a)[(1+e)^{-3} - (1-e)^{-3}] \tag{19a}$$

$$\overset{0\to\pi}{\Delta e} = 1/2.(\overset{0\to\pi}{\Delta a}/a).(1/e - e) \tag{19b}$$

The change in other parameters such as ω and i are not necessary. Here, these corrections reduce error in the true value of h_{AT} from about 0.5% to nearly 0.005%.

For any given trajectory, the transfer orbit parameters are obtainable from the final states of the 4th stage (Eqs. 20). Consequently, V_{AT}, i_T, and therefore J can be calculated. Eqs. (17, 18) mean that to have the maximum mass in the primary orbit, we desire to have a trajectory with the best combination of:

- Maximum mass in T.O. (i.e. minimum fuel consumption up to a burnout of the 4^{th} stage)
- Maximum perigee height for T.O. (to increase V_{AT})
- Minimum inclination for T.O.

Initial Conditions

The control during the first stage is the gravity turn program and so the thrust vector is parallel to the velocity vector (i.e. zero thrust angles). After the lift-off, the vehicle is vertically flown for 10 s to leave the launch site. The vehicle then pitches slowly to differ from the vertical state. Gravity turn trajectories of a given launching vehicle belong to a family of ascent trajectories that all start from the vertical flight ($\gamma = 90°$) and at a subsequent point of time $t = t_G$ has a specific flight path angle $\gamma(t_G)$. At $t = t_G$, there is only one and only one value of $\gamma(t_G)$ for each trajectory in the family. At this moment of time, the flight path angle determines the further trajectory of the vehicle and so $\gamma(t_G)$ acts as a boundary condition to specify the trajectory. In the case of Europa-II, it is useful to choose:

$$t_G = t_0 + 20\,s, \tag{20}$$

Therefore, the only parameter to be optimized at the first stage can be chosen as:

$$\phi_G = \phi(t_G) = 90° - \gamma(t_G). \tag{21}$$

As described in [1], it is possible to determine the family of trajectories for the carrier as a function of ϕ_G in the time interval $[t_0, t_G]$. So, the left hand boundary

Table 5. Initial Conditions at $t=t_G$

θ_0(deg)	δ_0(deg)	r_0(m)	V_0(m/s)	χ_0(deg)	γ_0(deg)	Q_0(J/cm^2)	m_0(kg)
0	5.2366	R_E+512.84	Eq.(22)	91.6	90°-ϕ_G	44.7186	101115.718

for integration of state equations is t_G, while the initial conditions are dependent on the parameter ϕ_G. The range of interest for ϕ_G is 0.1° to 1.5°. Because of the short period of the motion up to t_G, it is expected that most initial conditions have a mean value that does not change for different values of ϕ_G. In fact, calculations show that this is true except for V (and of curse for γ). Initia1 conditions are listed in Table(4). The velocity can be very well approximated by:

$$V(\phi_G) = b_0 + b_2\phi_G^2 + b_4\phi_G^4 + b_6\phi_G^6 \qquad (22)$$

$\phi_G : (deg), V : (m/s).$

Final Conditions

The necessary conditions for entry to the transfer orbit are:

$$V_i^2 = \mu(2/r - 1/a_T) \rightarrow P_1 \equiv 1/a_T = 2/r - V_i^2/\mu \qquad (23a)$$

$$r_{AT} = a_T(1 + e_T) \rightarrow P_2 \equiv e_T = P_1 r_{AT} - 1 \qquad (23b)$$

$$r = a_T(1 - e_T^2)/(1 + e_T \cos\nu_T) \rightarrow$$
$$P_3 \equiv \cos\nu_T = [(r_{AT}/r)(1 - P_2) - 1]/P_2 \qquad (23c)$$

$$\tan\gamma_i = (e_T \sin\nu_T)/(1+e_T \cos\nu_T) \rightarrow$$
$$1 - P_3^2 = \tan^2\gamma_i(1/P_2 + P_3)^2 \qquad (23d)$$

Since the perigee of the transfer orbit should be in the equatorial plane, another condition is required:

$$\left.\begin{aligned} -\sin\nu_T.\sin i_T &= \sin\delta \\ \cos i_T &= \cos\delta\sin\chi_i \end{aligned}\right\} \rightarrow (1-P_3^2)(1-\cos^2\delta\sin^2\chi_i) = \sin^2\delta \qquad (23e)$$

In these equations, P_1, P_2 and P_3 are new parameters to define transfer orbit entrance conditions efficiently in the nonlinear programming (NLP) representation of the problem. It is a good idea to use some auxiliary parameters to break down the relations between a set of equations (conditions) to simplify the calculation of derivatives. These parameters are appropriately bounded for better convergence.

In the case of attachment at perigee point, these conditions are simplified by putting ν=0. It is clear that this leads to $\delta = \gamma$ =0.

Table 6. Coefficients of Eq.(22)

b_0(m/s)	b_2(m/s.deg^2)	b_4(m/s.deg^4)	b_6(m/s.deg^6)
55.931147	3.63618187E-3	-9.98226111E-7	2.33384110E-7

Other Conditions

During the ascent, internal conditions specified by Eqs. (2b), (3a) and path constraints specified by Eqs. (3b), (4) should also be satisfied by the vehicle.

SOLUTION

This control and parameter optimization problem is solved by means of a direct collocation method and nonlinear programming. The internal NLP solver used here is IPOPT [7], an interior point algorithm for large-scale nonlinear optimization. The inequality constraints should be reformulated as equality constraints by means of slack variables. Since some of the state parameters such as r have very large values while others such as attitude angles have very small values, states and controls are all scaled to the similar intervals near [-0.5,0.5] to improve solution efficiency and numerical considerations described in [8]. Differential equations of the motion are reformulated as equality constraints (defects) and constitute the main part of the constraints. The first derivative information required by the NLP solver is determined analytically except when it was not possible or was too difficult. In those cases, a 2^{nd} order finite difference method is used. Defect equations for trapezoidal collocation scheme are:

$$C_i^k \equiv X_i^{k+1} - [X_i^k + 1/2(f_i^k + f_i^{k+1})h_i^k] = 0 \qquad (24)$$

where subscripts are due to the states (and controls) at each grid point and superscripts specify the grid indices in the time domain. For detailed information about direct collocation method see [8,11]. To determine sparsity pattern of the Jacobean matrix, derivatives of state equations with respect to the states (∂f/∂x) are

Table 7. Results for Different Conditions

Case	Condition	$\phi^*_{(G)}$(deg)	t_{f4}(s)	t_s (s)	i_C (deg)	i_T (deg)	ν_T(deg)	h_{PT}(km)	m_P(kg)
A	Attach to Perigee of T.O.	1.1985	1508.1	234.6	4.995	3.570	0	324.6	237.149
B	Free Attachment to T.O.	1.1985	1882.2	237.2	4.997	3.591	7.169	440.7	238.088
B′	Ref. [1], (Traj. # 21)	1.1984	1885.9	237.3	4.998	3.604	N/A	441.8	238.092
C	Heating Index C_1 = 160 kJ/cm^2	1.2597	1890.1	255.2	4.994	3.593	7.418	454.6	238.201

analytically determined and inserted into the program code. The second derivatives (Hessian information) are not treated in this manner and IPOPT is asked to use its numerical approximation methods for them.

The problem is discretized as shown in Figure (3a) up to burnout of the 4^{th} stage. The defects which link the values of states between each two grid points through Eq. (24) are shown in Figure (3b). There are special grid nodes at boundaries of stages to introduce connect conditions between the different phases such as the mass-drops and the effect of the short free flight delay before ignition of a new stage. For a detailed discussion on the formulation of multi-phase problems see [9].

Since the control vector at the first stage is zero, and the coast phase does not have any thrust (i.e. no control is defined), the trajectory for these phases can be integrated as an ODE initial value problem. However, to reduce the sensitivity of the solution to the initial guess and also to apply the path constraint specified by Eq. (3b) during the free flight phase, these parts of trajectory are also discretized (collocated). It is also possible to add only a few grid points that are related to each other from the ODE integration of state equations as in multiple shooting methods [10,11].

Nevertheless, it is important to have a grid at the end of the 4^{th} stage such that T.O. entrance conditions and their derivatives can be calculated efficiently.

The problem is discretized by 2000 grids for all conditions with a proper concentration at each phase. Due to the existence of aerodynamic forces, the first stage contains a relatively high number of grids with respect to its duration. Numerical solutions show that this amount of nodes is completely enough, and results do not change by increasing the nodes.

For an initial guess, a very simple linear approximation of states and zero (constant) values for controls are completely enough as shown in Table 6. The program converges quickly in all conditions (depending on the condition, about 60 to 80 iterations).

Results and Discussion

Table 7 lists important parameters from the results for 3 different conditions. In case A, it is assumed that the trajectory is attached to the T.O. at its perigee. As already stated, the necessary final conditions are too simple for this condition.

The optimal attachment point is determined in case B. It can be seen from Table 7 that it is about 7 deg after the perigee point and This condition improves the performance index (m_P) by nearly 0.94 kg. It should be noted that this amount of fuel saving increases the life-time of the satellite for about 2.86 months. For this condition, the results are compared with available values from [1] specified by B′ which are obtained by an indirect multiple shooting method with an inner loop for parameter optimization. Conditions used for case B′ from [1] are same as conditions used for case B of this work.

The effect of increasing the heating index is presented in C (see also Figs. 11, 12). For this condition, a free attachment point is also assumed. The gain in the payload is about 0.1 kg, which is not great with respect to the temperature rise of critical points of the vehicle, i.e, 37°C (Table 2). This shows that the current heating index is high enough.

Figure 4 shows the ascent trajectory up to the entry of the T.O. for case B (free attachment). The ground projection and vertical projection of the trajectory is also drawn. By comparing ground projections of T.O. and C.O. with respect to the equatorial line (latitude=0), it is possible to determine the inclination angles of these orbits. From Table 7, it can be seen that the optimal inclination of coast arcs are approximately the same for different conditions ($i_C \approx 5°$ and $i_T \approx 3.6°$).

Figure 5 shows the altitudes of trajectories vs the relative longitude. All trajectories are inserted into the C.O. before perigee point ($\gamma<0$) and as such, have a slight descent during the coast phase next to the third stage. For case A, the final part of the trajectory is turned to the horizontal direction as it attempts to attach to the perigee of transfer orbit (i.e. $\gamma=0$). This change of velocity vector direction requires an amount of energy, which why the performance is decreased in this case.

The velocities are relatively near each other up to the end of the third stage (Figure 6). The maximum final velocity is V_{f4}= 9662.0 m/s for case A and the minimum is V_{f4}= 9524.6 m/s for case C. It should be noted that a small change in the vehicle velocity requires a relatively large amount of energy (proportional by V^2).

Figure 7 shows the azimuth angles. The launch azimuth is limited to 91.6° in the first stage. It can be seen that the thrust force in the 4^{th} stage tries to decrease the azimuth angle as much as possible (i.e.$\chi \rightarrow 90°$). It changes the vehicle trajectory direction from i_C to i_T. As already stated, the smaller values for i_T are desirable (Eq. 18). From Figure 8, the flight path angle decreases rapidly from 90° to about 17° at the end of the first stage. Since attachment to both

Table 8. Initial Guess for States and Controls

θ	δ	r	V	χ	γ	Q	m	σ	ϵ
$\theta_0 \rightarrow$ 90°	$\delta_0 \rightarrow$ -1°	$r_0 \rightarrow R_E$+350 km	$V_0 \rightarrow$ 9500 m/s	91.6°	$\gamma_0 \rightarrow$ 0°	$Q_0 \rightarrow C_1$	use $\dot{m}_{Fuel}$	0°	0°

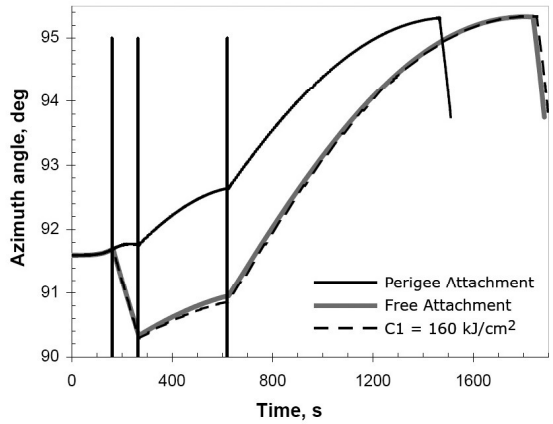

Figure 7. Azimuth angle vs time

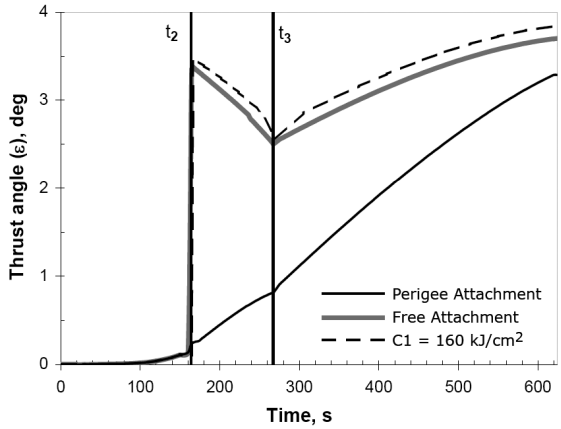

Figure 10. Thrust angle (ε) vs time

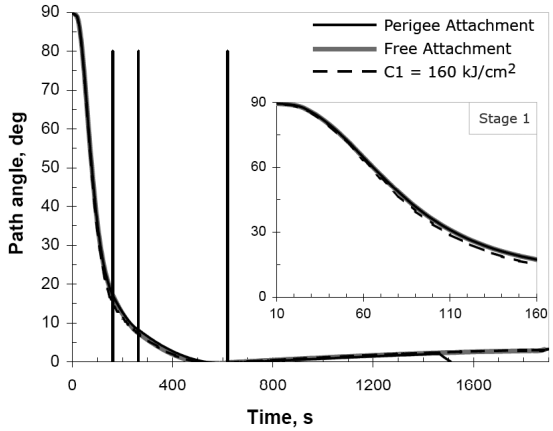

Figure 8. Flight path angle vs time (A, D)

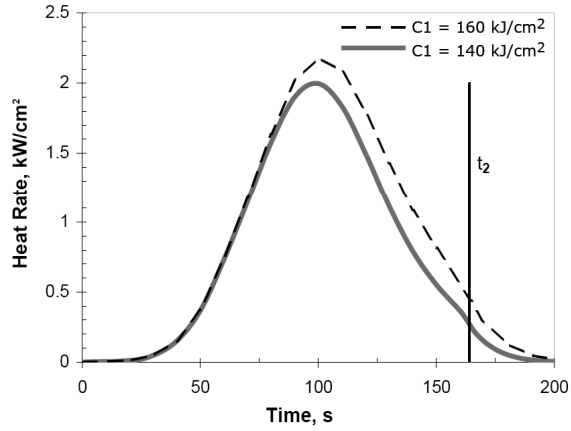

Figure 11. Heat rate (Aerothermal flux)

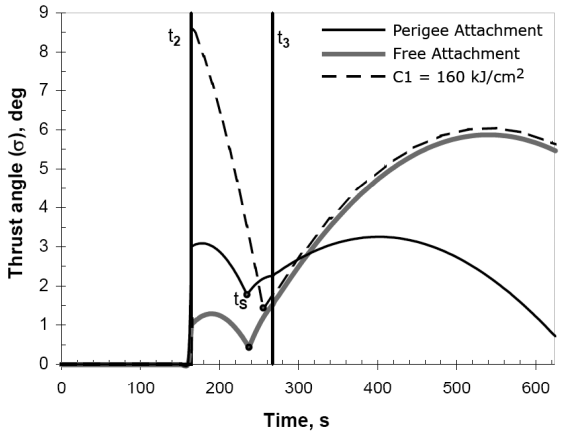

Figure 9. Thrust angle (σ) vs time

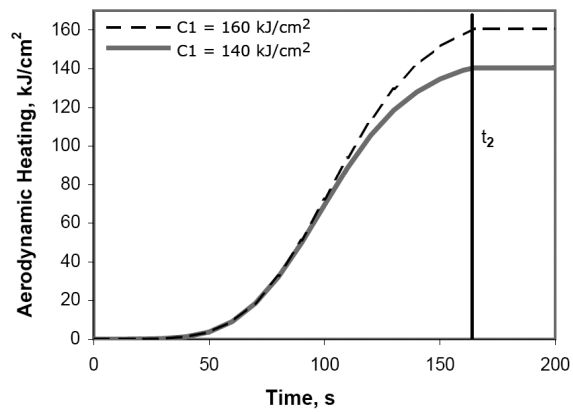

Figure 12. Time integral of aerothermal flux

C.O. and T.O. should occurr near the perigee points of these orbits, the flight path angle is approximately constant from the burnout of the 3^{rd} stage (i.e. entry to C.O.) to the burnout of the 4^{th} stage (i.e. entry to the transfer orbit). The value of γ at insertion to C.O. is -0.35° for case A and -0.18° for case C. Its value at its insertion into T.O. is 0 for case A and 3.18° for case C.

The optimal thrust direction angles (σ, ϵ) are shown in Figs. 9 and 10. At the first stage, σ is 0 while ϵ is required to have very small values to keep the vehicle in the specified Earth-fixed plane.

CONCLUSION

This work shows that by using direct collocation and non- linear programming method, we can find good solution of this optimal control and parameter optimization problem without the difficulties usually arising from indirect methods such as definition of switching structures for constrained arcs or generation of a good initial guess (specially for adjoint variables which do not have any physical meaning) for convergence. However, in the present work, the solution converges using a very simple initial guess (zero for controls and piecewise-linear or linear estimation for states).

In addition, It is easy to force states and controls to remain in prescribed bounds which may help the program to avoid nonphysical values.

Another advantage of the present work over that of [1] is the following: It can find optimal values for all parameters, whereas the method of [1] could not find the optimal value of i_T (due to convergence difficulties arising from the complicated coupling of the parameters on the performance index), and so the program should find optimal trajectories based on different values of i_T for each condition, and then choose the best values.

ACKNOWLEDGMENTS

The authors would like to express their appreciation to A. Watcher for providing IPOPT and for his illuminating discussions in regard to use this package.

REFERENCES

1. Duffek, W., and Shau, G. C., "Optimierung der aufstiegsbahn eines 4stufigen tragers fur synchronbahnmissionen", Institute for the Dynamics of Flight Systems, Department: Flight Trajectories, Germany, (1974).
2. C.J. Riley, F.R. DeJearnette, "Engineering Aerodynamic Heating Method for Hypersonic Flow", *Journal of Spacecraft and Rockets*, **29(3)**, (1992).
3. Park, S. Y., "Launch Vehicle Trajectories with a Dynamic Pressure Constraint", *Journal of Spacecraft and Rockets*, **35(6)**, (1998).
4. Seyed aghajan, M., "Trajectory Optimization of Multistage Rockets", M.Sc. Thesis, Aerospace Engineering Deptartment, Amirkabir University of Technology.(1378).
5. , "U.S. Standard Atmosphere, 1962", U.S. Government Printing Office, Washington DC., (1962).
6. Kozai, Y., "The Motion of a Close Earth Satellite", *the Astronomical Journal*, **64**, PP 367-377(1959).
7. Waechter, A. and Biegler, L. T.,, "On the Implementation of an Interior-Point Filter-Line Search Algorithm for Large-Scale Nonlinear Programming", *Research Report RC 23149*, IBM T.J. Watson Research Center, Yorktown, NY, USA, (2004).
8. Betts, J. T., "Methods for Optimal Control Using Nonlinear Programming", SIAM (Society for Industrial and Applied Mathematics), Philadelphia, (2001).
9. Jansh, C., Schnepper, K., Well, K. H., " Multiphase Trajectory Optimization Methods with Applications to Hypersonic Vehicles", *Applied Mathematics in Aerospace Science and Engineering*, Miele, A., Salvetti, A., ed., Plenum Press, New York, (1994).
10. Calise, A. J., Tandon, S., Young, D. H., "Further Improvements to a Hybrid Method for Launch Vehicle Ascent Trajectory Optimization", *AIAA-2000-4261*, AIAA Guidance, Navigation, and Control Conference, (2000).
11. Gath, P. F., Well, K. H., "Trajectory Optimization Using a Combination of Direct Multiple Shooting and Collocation", *AIAA 001-4047*, AIAA Guidance, Navigation, and Control Conference, Montreal, Quebec, Canada, (6-9 August 2001).